J|A|C|S
ARTICLES
Published on Web 12/07/2006

Diastereomeric Xe Chemical Shifts in Tethered Cryptophane Cages

E. Janette Ruiz,[†,#] Devin N. Sears,[‡,§] Alexander Pines,[†] and Cynthia J. Jameson*[,‡]

Contribution from the Department of Chemistry, University of California at Berkeley, Berkeley, California 94720, Material Sciences Division, Lawrence Berkeley National Laboratory, Berkeley, California 94720, and the Department of Chemistry, University of Illinois at Chicago, Chicago, Illinois 60607

Received September 14, 2006; E-mail: cjjames@uic.edu

Abstract: Cryptophane cages serve as host molecules to a Xe atom. Functionalization of cryptophane-A has permitted the development of Xe as a biosensor. Synthetic routes used to prepare cryptophanes result in racemic mixtures of the chiral cages. In the preparation of a tethered cryptophane-A cage for biosensor applications, some achiral and chiral substituents such as left-handed amino acids have been used. When the substituent is achiral, the NMR signal of the Xe atom in the functionalized cage in solution is a single isotropic peak, since the Xe shielding tensor components in the **R** and **L** cages differ by no more than the signs of the off-diagonal elements. Chiral substituents can split the cage-encapsulated Xe NMR signal into one or more sets of doublets, depending on the number of asymmetric centers in the substituent. We carry out quantum mechanical calculations of Xe nuclear magnetic shielding for the Xe atom at the same strategic position within an **L** cryptophane-A cage, under the influence of chiral potentials that represent **r** or **l** substituents outside the cage. Calculations of the Xe shielding response in the **Lr** and **Ll** diastereomeric pairs permit the prediction of the relative order of the Xe chemical shifts in solutions containing the **Rl** and **Ll** diastereomers. Where the substituent itself possesses two chiral centers, comparison of the calculated isotropic shielding responses in the **Ll**$_{r}$, **Lr**$_{l}$, **Rl**$_{l}$, and **Lr**$_{r}$ systems, respectively, permits the prediction of the Xe spectrum of diastereomeric systems in solutions containing **Ll**$_{r}$, **Rl**$_{r}$, **Ll**$_{l}$, and **Rl**$_{l}$ systems. Assignment of the peaks observed in the experimental Xe NMR spectra is therefore possible, without having to undertake the difficult synthetic route that produces a single optically pure enantiomer.

I. Introduction

Cryptophanes constitute an important class of host molecules.[1,2] The chiral anti isomers have received particular interest because of their ability to achieve chiral recognition.[3−6] A Xe atom as a guest in smaller cryptophanes in organic solution has generated a great deal of interest. In particular, the extreme sensitivity of the Xe chemical shifts in these quasi-spherical cages to cage size, temperature, and degree of deuterium substitution has been demonstrated.[7−12]

The affinity of Xe for hydrophobic cavities in macromolecular interiors has motivated a variety of applications of this inert gas in biochemical and structural studies in proteins,[13−16] in cells,[17,18]and in tissues.[19−21] Wemmer, Pines, et al. have been developing ^{129}Xe NMR as a tool for detecting protein cavities

[†] University of California at Berkeley and Materials Sciences Division, Lawrence Berkeley National Laboratory.
[‡] University of Illinois at Chicago.
[§] Current address: Department of Chemistry, University of Alberta, Edmonton, Alberta T6G 2G2 Canada.
[#] Current address: Lam Research Corp., P.O. Box 5010, Fremont, CA 94536.

(1) Collet, A. In *Comprehensive Supramolecular Chemistry;* Atwood, J. L., Davis, J. E. D., MacNicol, D. D., Vogtle, F., Eds.; Pergamon: New York, 1996; Vol. 2, Chapter 11, pp 325−365.
(2) Collet, A. *Tetrahedron* **1988**, *43*, 5725−5759.
(3) Canceill, J.; Lacombe, L.; Collet, A. *J. Am. Chem. Soc.* **1985**, *107*, 6993−6996.
(4) Costante-Crassous, J.; Marrone, T. J.; Briggs, J. M.; McCammon, J. A.; Collet, A. *J. Am. Chem. Soc.* **1997**, *119*, 3818−3823.
(5) Costante, J.; Garcia, C. Collet, A. *Chirality* **1997**, *9*, 446−453.
(6) Tambute, A.; Canceill, J.; Collet, A. *Bull. Chem. Soc. Jpn.* **1989**, *62*, 1390−1392.
(7) Bartik, K.; Luhmer, M.; Dutasta, J. P.; Collet, A.; Reisse, J. *J. Am. Chem. Soc.* **1998**, *120*, 784−791.
(8) Luhmer, M.; Goodson, B. M.; Song, Y. Q.; Laws, D. D.; Kaiser, L.; Cyrier, M. C.; Pines, A. *J. Am. Chem. Soc.* **1999**, *121*, 3502−3512.
(9) Brotin, T.; Lesage, A.; Emsley, L.; Collet, A. *J. Am. Chem. Soc.* **2000**, *122*, 1171−1174.
(10) Brotin, T.; Devic, T.; Lesage, A.; Emsley, L.; Collet, A. *Chem.—Eur. J.* **2001**, *7*, 1561−1573.
(11) Brotin, T.; Dutasta, J. P. *Chem.—Eur. J. Org. Chem.* **2003**, 973−984.
(12) Spence, M. M.; Rubin, S. M.; Dimitrov, I. E.; Ruiz, E. J.; Wemmer, D. E.; Pines, A.; Yao, S. Q.; Tian, F.; Schultz, P. G. *Proc. Natl. Acad. Soc. U.S.A.* **2001**, *98*, 10654−657.
(13) Schoenborn, B. C.; Watson, H. C.; Kendrew, J. C. *Nature* **1965**, *207*, 28−30.
(14) Montet, Y.; Amara, P.; Volbeda, A.; Vernede, X.; Hatchikian, E. C.; Field, M. J.; Frey, M.; Fontecilla-Camps, J. C. *Nat. Struct. Biol.* **1997**, *4*, 523−526.
(15) Wentworth, P., Jr.; Jones, L. H.; Wentworth, A. D.; Zhu, X.; Larsen, N. A.; Wilson, I. A.; Xu, X.; Goddard, W. A., III; Janda, K. D.; Eschenmoser, A.; Lerner, R. A. *Science* **2001**, *293*, 1806−1811.
(16) Whittington, D. A.; Rosenzweig, A. C.; Frederick, C. A.; Lippard, S. J. *Biochemistry* **2001**, *40*, 3476−3482.
(17) Bifone, A.; Song, Y. Q.; Seydoux, R.; Taylor, R. E.; Goodson, B. M.; Pietrass, T.; Budinger, T. F.; Navon, G.; Pines, A. *Proc. Natl. Acad. U.S.A.* **1996**, *93*, 12932−12936.
(18) Wolber, J.; Cherubini, A.; Leach, M. O.; Bifone, A. *Magn. Reson. Med.* **2000**, *43*, 491−496.
(19) Swanson, S. D.; Rosen, M. S.; Coulter, K. P.; Welsh, R. C.; Chupp, T. E. *Magn. Reson. Med.* **1999**, *42*, 1137−1145.
(20) Duhamel, G.; Choquet, P.; Grillon, E.; Lamalle, L.; Leviel, J. L.; Ziegler, A.; Contantinesco, A. *Magn. Reson. Med.* **2001**, *46*, 208−212.

 10.1021/ja066661z CCC: $33.50

that bind xenon and have been using Xe chemical shifts as a reporter of cavity structure in proteins in solution, as well as in crystals.[12,22,23] Although the Xe chemical shifts in cavities can potentially provide signatures of protein cavity structure, two important limitations to the feasibility of Xe chemical shifts in protein solutions as protein assays are (a) the cavity structure is not unique to a specific protein and (b), even in those cases where the nature of the cavity is uniquely associated with a specific protein, the Xe residence time in the protein cavity is not sufficiently long for the site-specific chemical shift to be observed. Only the exchange-averaged Xe chemical shift in solution can be obtained, and its dependence on the protein concentration is not sufficiently unique for identification purposes.

The sensitivity advantage of hyperpolarized Xe combined with the functionalization of cryptophanes has made it possible to develop a family of compounds with potential as biosensors.[12,23,24] Furthermore, the sensitivity of biosensor-encapsulated xenon to its local environment indicates that functionalized xenon can serve as a magnetic resonance reporter not only for targeted in situ biosensing, but also for imaging.[25] In the proof-of-concept example of biosensor activity, binding of a biotin-derivatized cage to avidin leads to a shift of the signal of the encapsulated Xe to higher chemical shift.[12,23,24] Understanding the Xe chemical shifts which provide the biosensor capability would be useful, especially for the development of desired multiplexing capability described as many different cages recognizing many different proteins in a single solution. In our previous work,[26] use of a quantum mechanical description of the Xe shielding response to a cryptophane cage in conjunction with statistical mechanical averaging over the possible Xe configurations within the cage has yielded a quantitative understanding of the sensitivity of the isotropic Xe chemical shift in various cryptophane cages, including the observed dependence on cage size, isotopic substitution, and temperature. A combination of molecular dynamics and Monte Carlo simulations permitted us to predict the chemical shift of the encapsulated Xe atom, upon binding of the biosensor to the protein, entirely on the basis of mechanical deformation of the cage tethered to the binding site at a protein which is largely immobile. Any mechanical deformation that tends to flatten a nearly spherical cage, even slightly, diminishes the effective internal volume available to the Xe, thus leading to a larger chemical shift when the binding event occurs. The shape of the Xe shielding response function, particularly the way that the function changes sharply upon close approach to neighbors, leads to the extreme sensitivity of the average Xe chemical shift to the size and shape of the confining space. In turn, it is this exquisite sensitivity to any changes in the dimensions of the cage that allows consideration of mechanical deformation alone to accurately provide simple predictions of the directional change of the Xe chemical shift upon binding to the protein.[26] This model is completely consistent with the recent experimental observations that biosensor shifts are of the same sign independent of tether and linker length and consistent also with the larger Xe shifts upon binding when the linker is shorter, both of which have recently been observed.[24]

In this paper, we consider an interesting complication that arises from the sensitivity of Xe as a probe: the response of the Xe atom to its chiral environment and the observable consequences in its nuclear shielding. The synthetic routes used in preparing cryptophanes result in racemic mixtures of the chiral cages.[3−6] In the preparation of a tethered cryptophane-A cage for development of Xe as a biosensor, additional chemical groups, some chiral and some achiral, are introduced.[12, 23] When the substituent functional group is achiral, the NMR signal of the Xe atom in the functionalized cage in solution consists of a single isotropic peak since the Xe shielding tensor components in the **R** and **L** cages differ by no more than the signs of the off-diagonal elements. This observation is indeed predicted by quantum mechanical calculations of the Xe shielding tensor for Xe atoms in helices of Ne atoms.[27−30] In the characterization of the precursors involving chiral substituents using hyperpolarized Xe NMR, it was found that the Xe signal is split into one or more sets of doublets, depending on the number of asymmetric centers in the substituent.[31] This was the first report of the detection of diastereomers by a xenon atom. Since the parent cage was available only as a racemate (**R**/**L**), using an **l**−handed group to functionalize the cage produces both **Rl** and **Ll** in equal quantities. The diastereomeric splitting is preserved when the biosensor binds to the protein.[24] Although each member independently shifts when the sensor binds to the protein, the binding event shifts the two peaks in the same direction, but not necessarily by exactly equal amounts.

There had been earlier reports by Bartik et al. of splitting of the Xe NMR signal for the Xe atom in a solution of racemic cryptophane-A in the presence of the chiral chemical shift reagent, tris[3-(heptafluoropropylhydroxymethylene)-(+)-camphorato] europium (III).[32,33] In this case, the splitting largely arises from the different local hyperfine fields at the Xe position resulting from the unpaired electron-spin center in the right-handed europium complex. Although the authors had used an enantiopure cryptophane-A in one of their samples, they did not identify whether it was **R** or **L**, and the two peaks observed were not assigned. The local hyperfine field mechanism for the chemical shift is in addition to, and is not related to the differences in Xe shielding response that are observed in diastereomers. In fact, it is by neglecting the differences in shielding response for diastereomers that the lanthanide shift reagents may be applied to quantitative structure determination. Thus, the fact that Xe encapsulated in the enantiopure cage

(21) Wolber, J.; McIntyre, D. J. O.; Rodrigues, L. M.; Carnochan, P.; Griffiths, J. R.; Leach, M. O.; Bifone, A. *Magn. Reson. Med.* **2001**, *46*, 586−591.
(22) Rubin, S. M.; Lee, S. Y.; Ruiz, E. J.; Pines, A.; Wemmer, D. E. *J. Mol. Biol.* **2002**, *322*, 425−440.
(23) Spence, M. M.; Ruiz, E. J.; Rubin, S. M.; Lowery, T. J.; Winssinger, N.; Schultz, P. G.; Wemmer, D. E.; Pines, A. *J. Am. Chem. Soc.* **2004**, *126*, 15288−15294.
(24) Lowery, T. J.; Garcia, S.; Chavez, L.; Ruiz, E. J.; Wu, T.; Brotin, T.; Dutasta, J. P.; King, D. S.; Schultz, P. G.; Pines, A.; Wemmer, D. E. *ChemBioChem* **2006**, *7*, 65−73.
(25) Lowery, T. J.; Rubin, S. M.; Ruiz, E. J.; Spence, M. M.; Winssinger, N.; Schultz, P. G.; Pines, A.; Wemmer, D. E. *Magn. Reson. Imaging* **2003**, *21*, 1235−1239.
(26) Sears, D. N.; Jameson, C. J. *J. Chem. Phys.* **2003**, *119*, 12231−12244.
(27) Sears, D. N.; Jameson, C. J.; Harris, R. A. *J. Chem. Phys.* **2003**, *119*, 2685−2690.
(28) Sears, D. N.; Jameson, C. J.; Harris, R. A. *J. Chem. Phys.* **2003**, *119*, 2691−2693.
(29) Sears, D. N.; Jameson, C. J.; Harris, R. A. *J. Chem. Phys.* **2003**, *119*, 2694−2701.
(30) Sears, D. N.; Jameson, C. J.; Harris, R. A. *J. Chem. Phys.* **2003**, *120*, 3277−3283.
(31) Ruiz, E. J.; Spence, M. M.; Rubin, S. M.; Wemmer, D. E.; Pines, A.; Winssinger, N.; Tian, F.; Yao, S. Q.; Schultz, P. G. Presented at the 43rd Experimental NMR Conference, Asilomar, CA, April 14−19, 2002.
(32) Bartik, K.; El Haouaj, M.; Luhmer, M.; Collet, A.; Reisse, J. *ChemPhysChem* **2000**, *1*, 221−224.
(33) Bartik, K.; Luhmer, M.; Collet, A.; Reisse, J. *Chirality* **2001**, *12*, 2−6.

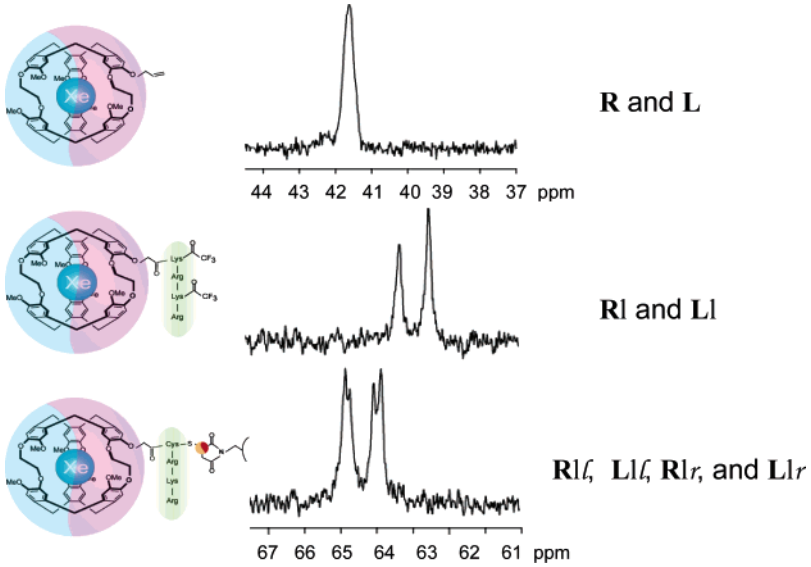

Figure 1. Detection of cage diastereomers by Xe chemical shift. The hyperpolarized Xe NMR spectrum of allyl substituted cryptophane-A in 25% toluene/75% tetrachloroethane (top) shows only one peak corresponding to both the **L** and **R** cage in the racemic mixture. The cage functionalized with a single enantiomer (**l**) peptide chain leads to a mixture of the chiral combinations **Rl** and **Ll** and correspondingly two Xe resonances separated by 0.84 ppm. The Xe spectrum after adding the biotin linker (truncated in the structural formula) shows four lines (bottom). A new racemic chiral center is formed at the connection involving the Cys residue and the prochiral maleimide. As a result, the cage−peptide−maleimide product is now a mixture of the chiral combinations **Rl𝓁**, **Ll𝓁**, **Rl***r*, and **Ll***r*. Color highlighting is used in this and the following figures to differentiate enantiopure (single color) and racemic (two color) components.

complexed by the shift reagent appears at higher chemical shift because of the local hyperfine fields caused by the electron spin does not offer any insight into the magnitudes or the signs of the differential shielding response exhibited by the double peaks appearing upon substitution of the racemate cages with L amino acids.[23]

In this paper, we present additional experimental observations on the diastereomeric sets that provide definitive evidence of the induced chirality of the Xe atom. We present a theoretical prediction of the Xe shielding responses in selected precursors of the tethered biosensor for which the hyperpolarized Xe NMR spectra have been measured in solutions containing diastereomeric pairs; namely, compounds found in references 23, 24, and in the present work. A theoretical understanding of the observed diastereomeric splittings in the Xe NMR signal has to include an analysis of the electronic factors. Since we have already demonstrated that a chiral potential alone can produce significant diastereomeric splittings in the Xe NMR spectrum in model systems,[27, 30] we will use the theoretical results on the electronic factors alone to provide a basis for the assignments of the observed peaks to the individual members of the diastereomeric systems in the solution.

II. Experiments

All ^{129}Xe NMR spectra shown here were obtained at 83 MHz ($\nu(^1H)$ = 300 MHz, B_0 = 7.0 T) on a Varian Inova spectrometer. Natural abundance Xe (Isotec or Spectra Gases) was spin-polarized by laser-polarized Rb gas using a commercial polarizer (Amersham Health, Durham, NC) and was introduced into the sample using previously described methods,[23, 34] with polarizations of 1−5%. Experiments involving water-soluble cryptophane derivatives were carried out at nominally 298 K in D_2O or in deionized water, except where otherwise indicated. All chemical shifts shown in the figures were referenced by assigning the xenon resonance signal in solution to 195 ppm. Acquisition time was 1 s with a spectral width of 60 kHz using 90° pulses. Fourier-transformed spectra were processed with zero-filling and Gaussian line-broadening values of 2 Hz, typically. A description of the synthetic approach used for the precursors and biosensor in the figures has been published, with details included, in Supporting Information.[23]

Shown in Figures 1, 2, 3, and 4 are examples of detection of diastereomers by Xe chemical shifts. In Figure 1, the hyperpolarized Xe NMR spectrum of allyl substituted cryptophane-A in 25% toluene/75% tetrachloroethane (top) shows only one peak corresponding to both the **L** and **R** cages in the racemic mixture. The cage functionalized with a single enantiomer (**l**) peptide chain leads to a mixture of the chiral combinations **Rl** and **Ll** and, correspondingly, two Xe resonances separated by 0.84 ppm. After adding the biotin linker (truncated in the structural formula), the Xe spectrum shows four lines (bottom). A new racemic chiral center is formed at the connection involving the Cys residue and the prochiral maleimide. As a result, the cage−peptide−maleimide product is now a mixture of the chiral combinations **Rl𝓁**, **Ll𝓁**, **Rl***r*, and **Ll***r*. Color highlighting is used in this and the following figures to differentiate enantiopure (single color) and racemic (two color) components, where the highlighting covers the entire chiral portion of the molecule. An example similar to Figure 1 has been presented in an earlier report on diastereomers detected by Xe.[23] In Figure 2 the cage derivatized with water soluble (**l**) amino acids exhibits two peaks split by 1 ppm, corresponding to the diastereomers **Ll** and **Rl**. The diastereomeric splitting is reduced to 0.84 ppm when the primary amines of the lysine residues are modified with trifluoroacetic acid. In Figure 3, Xe detects the small change that occurs when the biotinylated cryptophane-A structure is slightly modified by the substitution of NH_2 by OCH_3 on the terminal arginine residue of the water-solubilizing (**l**) peptide. The fact that the biotin ligand itself is chiral does not affect the number (two) of distinct diastereomers, **Rl𝓁** and **Ll𝓁** for both compounds in this example. In Figure 4, the spectrum obtained for the basic precursor (top) has a splitting of 1 ppm compared to the spectra of three structurally related biosensors. Two structures differ in spacer length and the third has an additional chiral center but equal spacer length to the longer of the first two mentioned. In the short spacer molecule the lysine amine group is directly connected to the biotin ligand, while in the long spacer, a 14-atom spacer arm

(34) Han, S. I.; Garcia, S.; Lowery, T. J.; Ruiz, E. J.; Seeley, J. A.; Chavez, L.; King, D. S.; Wemmer, D. E.; Pines, A. *Anal. Chem.* **2005**, *77*, 4008−4012.

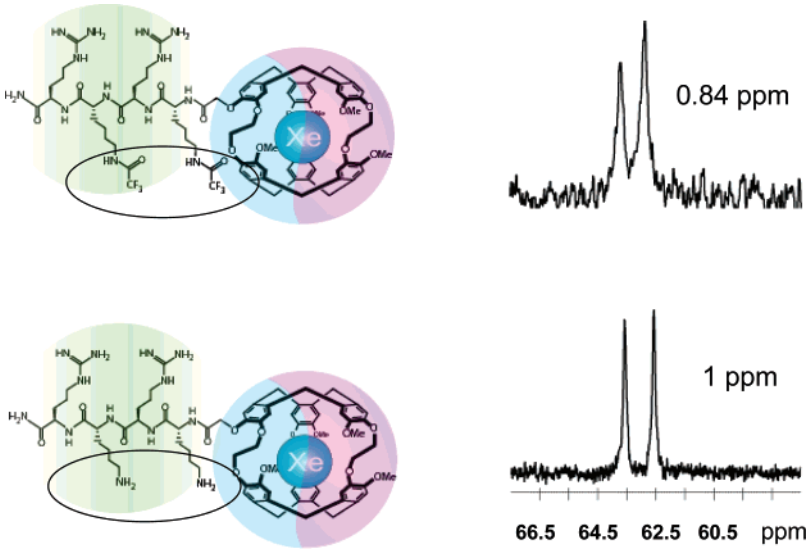

Figure 2. The cage derivatized with water soluble (**l**) amino acids exhibits two peaks split by 1 ppm, corresponding to the diastereomers **Ll** and **Rl**. The diastereomeric splitting is reduced to 0.84 ppm when the primary amines of the lysine residues are modified with trifluoroacetic acid.

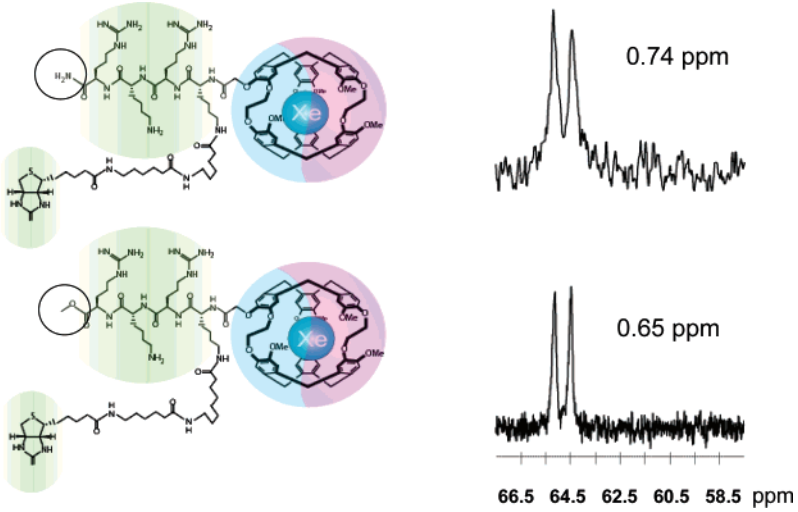

Figure 3. Xe detects the small change when the biotinylated cryptophane-A structure is slightly modified by the substitution of NH_2 by OCH_3 on the terminal arginine residue of the water-solubilizing (**l**) peptide. The fact that the biotin ligand itself is chiral does not affect the number of distinct diastereomers: **Rl**/ and **Ll**/ for both compounds.

connects the lysine amine group to the biotin. In the third molecule, the racemic spacer involves the Cys residue and the prochiral maleimide. The short and long spacers lead to diastereomeric splittings of 0.62 and 0.74 ppm, respectively. Inserting the Cys residue and the prochiral maleimide causes a finer splitting of each of the peaks shown in the spectrum just below. The absolute chemical shifts cannot be compared directly in these spectra because of the slightly different conditions of the Xe reference peak, sometimes in deionized H_2O, others in pure D_2O. The Xe chemical shift is extremely sensitive to such conditions. Assigning the Xe peak in solvent arbitrarily to 195 ppm leads the spectra in pure D_2O to appear to higher chemical shifts. Only the diastereomeric splittings should be compared in this work. Factors affecting the Xe line widths in the various biosensor systems and precursors have been discussed previously.[24]

III. Theoretical Approach and Methods

We show in Figure 5 the structure of the cryptophane-A cage that we used for the calculations. The symmetry is D_3. In the original classification by Collet,[1] cryptophane-A is composed of two cyclotriveratrylene caps (with crown structures of configuration M or P) oriented out−out in an anti arrangement, the enantiomers being designated M_oM_o and P_oP_o, where the subscripts correspond to out−out. The M_oM_o enantiomer has been found to have optical rotation $[\alpha]^{25}_D = -254$ in chloroform solution.[35] This is in good agreement with the recently measured optical rotation in $CHCl_3$ solution for the $P_oP_o(+)$ enantiomer ($[\alpha]^{25}_{589} = +269$).[36] The screw direction of the three $-OCH_2CH_2O-$ bridging groups is analogous to that of the **L** helix shown in Figure 5, so we may call the $M_oM_o(-)$ enantiomer of cryptophane-A cage the **L** enantiomer.

For the purpose of understanding the diastereomeric Xe shifts in the present work, we use quantum mechanical calculations of Xe shielding in the full cryptophane-A cage of chirality **L** under the influence of substituents which are represented by chiral potentials; that is, where only the charge distributions, not the explicit electrons of the substituents, are included. The Xe shielding is calculated for the all-electron Xe atom in the

(35) Canceill, J.; Collet, A.; Gottarelli, G.; Palmieri, P. *J. Am. Chem. Soc.* **1987**, *109*, 6454−6464.
(36) Brotin, T.; Barbe, R.; Darzac, M.; Dutasta, J. P. *Chem.—Eur. J.* **2003**, *9*, 5784−5792.

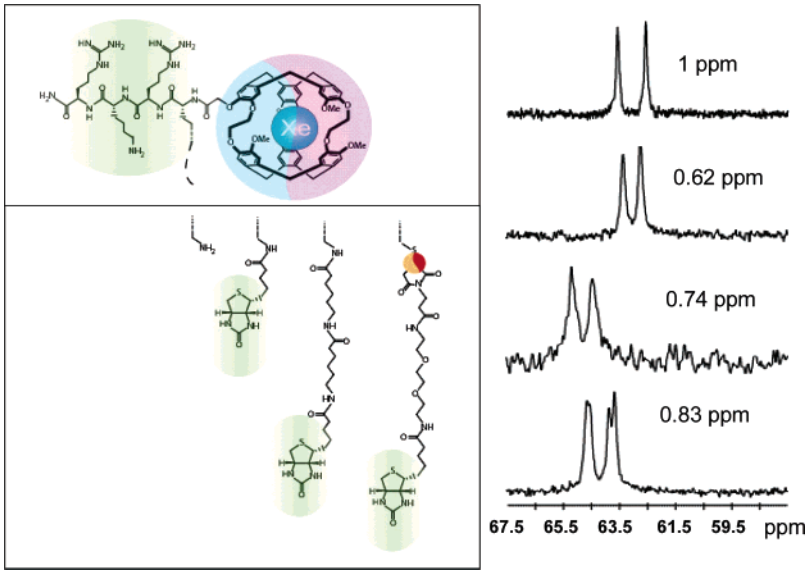

Figure 4. The spectra obtained for the basic precursor (top) and structurally related biosensors with short spacer (lysine amine group is directly connected to the biotin ligand), long spacer (a 14-atom spacer arm connects the lysine amine group to the biotin), and a racemic spacer (involving the Cys residue and the prochiral maleimide), respectively, completing the first lysine in the solubilizing peptide.

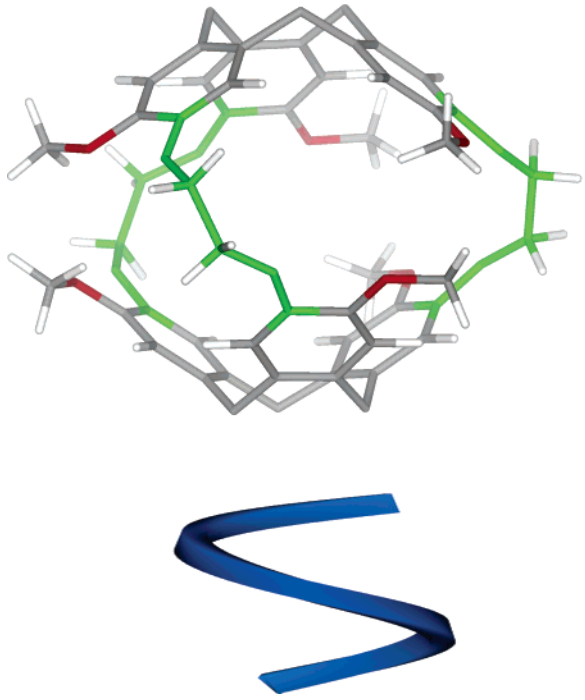

Figure 5. The $M_0M_0(-)$ enantiomer of the cryptophane-A cage. The **L** label used in the present work is consistent with the **L** label for the left-handed helix, as shown.

all-electron cryptophane cage, with the substituents represented in their proper spatial configuration by partial charges instead of atoms. This approach is based on our recent investigations of the shielding tensor of Xe and naked spins embedded in Ne helices,[27−30] where we found that a chiral potential alone can provide a diastereomeric shift that is sufficiently large, of the order of magnitude of the splittings observed experimentally for Xe.[23,31] In addition, by a general analysis of odd and even terms in both the potential and shielding, we found that the Xe peak assignment is associated only with the chirality of the partial charge potential, and the spatial geometry of the chiral potential is an important factor.[30] The assignment of the peaks is not affected by the absolute magnitudes or signs of charges used. In the approach used here, we are assuming that the **l** and **r** substituents do not result in *differential* mechanical deformation of the cage. In this way, the one-body distribution function of Xe within the cage is the same for each individual member of the diastereomeric system. With this assumption, the relative order of the calculated values of the Xe shielding response at a single selected point within the cage will be preserved in the relative magnitudes of the *average* Xe shielding responses in solution. The true average, of course, involves not only the Xe atom sampling the entire interior volume of the cage but also the dynamic averaging of cage and tether atoms in solution.

The **Rr** and **Ll** systems are mirror images and produce the same Xe shielding response; likewise the **Rl** and **Lr** systems are mirror images and produce the same Xe shielding response. We had verified these by theoretical calculations of Xe shielding responses in diastereomeric helical systems. Only the signs of the off-diagonal tensor components related by rotations in the molecular-coordinate frame differ for the respective mirror-image systems.[27] On the basis of these theoretical identity relations, we select individual chiral systems for theoretical study in the present work. Our theoretical calculations start with only **L** cages, and we prepare **Ll** and **Lr** systems in the computer. Experimentally, the diastereomers have been synthesized from a racemic mixture of **R** and **L** cages and enantiotopically pure **l** tether. We expect to find that we can unequivocally assign, from theory alone, the peaks in the Xe NMR spectrum of the set of diastereomers in solution—one specifically to **Ll** and the other one to **Rl** (theoretically the same Xe shielding as **Lr**). Where the substituent itself possesses two chiral centers, comparison of the calculated isotropic Xe shielding responses in the **Lr**$_{r,s}$, **Ll**$_{r,s}$, **Lr**$_{r,s}$, and **Ll**$_{r,s}$ systems, respectively, will provide the prediction of the experimental Xe spectrum of diastereomeric systems in solutions containing **Rl**$_{r,s}$, **Ll**$_{r,s}$, **Rl**$_{r,s}$, and **Ll**$_{r,s}$ systems. The specific diastereomeric systems for which the Xe shielding response calculations have been carried out in the present work are the two precursors shown in Figure 2 and also a truncated version of the biosensor shown in Figure 4. In the latter, a new

racemic chiral center is formed at the connection involving the Cys residue and the prochiral maleimide. We perform quantum calculations on the cage−peptide−maleimide product without the linker containing the biotin.

A. Determination of Geometries. Molecular mechanics molecular dynamics simulations in a liquid solvent are used in the present work to provide average spatial configurations of the **Lr** and **Ll** versions (for a series of functionalized cryptophane-A cages), and **Lr**$_{\curvearrowright}$, **Ll**$_{\curvearrowright}$, **Lr**$_{\nearrow}$, and **Ll**$_{\nearrow}$ systems (for a tether with more than one asymmetric center). For each system, the MD simulations optimize the geometry of the chiral substituent in solution while attached to a cryptophane-A cage filled with $CHCl_3$ that acts as surrogate for Xe. We had previously determined the minimum energy structure of a cryptophane-A cage that is occupied by a Xe atom at the center, using quantum mechanical geometry optimization.[26] The goal now is to determine the way in which the chiral substituent of the functionalized cage arranges itself around the cage in solution. The equilibrated tetrachloroethane solvent box to be used as the starting point for MD simulations of the solvated cryptophane-A/tether systems to be investigated was prepared at the experimental density by a combination of steepest-descent energy minimization and simulated annealing steps. The CFF91 force field was used throughout this study because, of the force fields available within Cerius[2] version 4.2 (MSI, San Diego, CA), it is the best suited for the types of molecular systems under investigation in the present work. We started with the average cryptophane-A geometry which had been generated by quantum mechanical geometry optimization and used in the theoretical study of xenon chemical shifts inside the cryptophane-A cage.[26] The appropriate number of solvent molecules of equivalent volume was removed from the equilibrated solvent box and the unequilibrated cryptophane-A/tether was placed into the simulation box with its coordinates initially frozen. The resulting cryptophane-A/tether structure from a series of simulated annealing and steepest-descent minimization procedures was then used as the input structure for a quantum mechanical calculation to obtain the partial atomic charges of the entire molecule.

B. Quantum Mechanical Calculations. All quantum mechanical shielding calculations were carried out with the PQS software package[37] using the gauge-including atomic orbitals (GIAO) choice of distributed origins.[38] The set of 240 basis functions on the Xe atom is the same one we have used previously for Xe intermolecular shielding response calculations.[26, 39−41] We have demonstrated in our previous work that the quality of the Xe basis set we are using leads to a very small counterpoise correction to the shielding response; for example, the difference in shieldings calculated for the free Xe atom using only the 240 basis functions of Xe and that calculated using also 1014 basis functions on half the cryptophane cage amounted to only 0.01 ppm.[26] The calculation of Löwdin charges for the functionalized cryptophane-A cage was carried out using DFT/B3LYP with a 6-31G* basis. We adopted the

(37) *PQS, version 3.1*; Parallel Quantum Solutions: 2013 Green Acres Road, Fayetteville, Arkansas 72703; 2004.
(38) Wolinski, K.; Hinton, J. F.; Pulay, P. *J. Am. Chem. Soc.* **1990**, *112*, 8251−8260.
(39) de Dios, A. C.; Jameson, C. J. *J. Chem. Phys.* **1997**, *107*, 4253−4270.
(40) Jameson, C. J.; Sears, D. N.; de Dios, A. C. *J. Chem. Phys.* **2003**, *118*, 2575−2600.
(41) Sears, D. N.; Jameson, C. J. *J. Chem. Phys.* **2003**, *118*, 9987−9989.

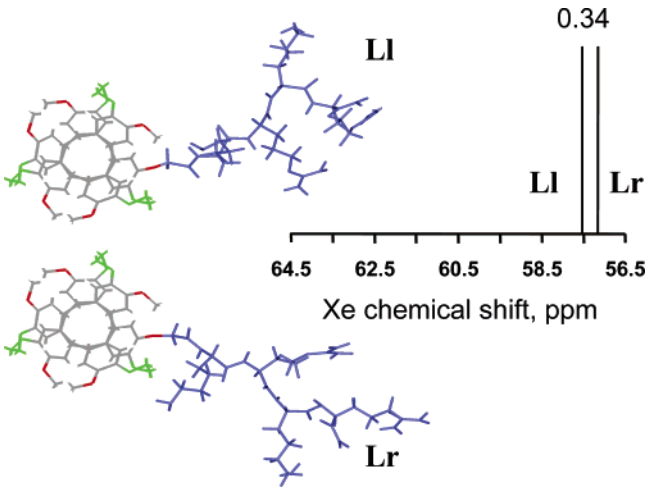

Figure 6. The Xe signals predicted for Xe in the (**L**) cage with (**l**) tether and (**r**) tether. The tether is the peptide lysine−arginine−lysine−arginine in the shown conformations for (**l**) and (**r**) forms, respectively, obtained by molecular dynamics simulations of each tethered cage in a solvent box.

Löwdin definition of the partial charges to generate the chiral potential that will represent the substituents, in part because the Löwdin definition permits a more realistic representation of the charge distribution than Mulliken populations, for example. Each atom in the substituent is replaced with a point charge equal to the calculated Löwdin partial charge. In the present work, the cryptophane cage atoms, arranged in the quantum-optimized geometry,[26] are described at the 6-31G* level, and the full 240 basis functions are used for the xenon atom, so that a calculation of the Xe shielding response in each member of the diastereomeric set requires 1752 basis functions. We selected a single "typical" position at which to locate the Xe atom within the cage for all the shielding response calculations in the present work. At this position within the unsubstituted cryptophane-A cage, the Xe atom has an isotropic Xe shielding response that is close to the average shielding, and the Xe atom also has a high probability of being found, on the basis of the one-body distributions functions resulting from Monte Carlo simulations in previous work.[26] The quantum mechanical (DFT/B3LYP) calculation of the Xe shielding response of a xenon atom in an **L** cryptophane-A cage is carried out in the presence of the unique spatial arrangement of Löwdin charges for each **r** or **l** substituent. Where the tether itself possesses two chiral centers, **r** or **l** and $_{\curvearrowright}$ or $_{\nearrow}$, we carried out calculations for the set of four Xe-distinguishable systems: **Lr**$_{\curvearrowright}$, **Ll**$_{\curvearrowright}$, **Lr**$_{\nearrow}$, and **Ll**$_{\nearrow}$ systems.

IV. Results

The results of the theoretical calculations are given in Figure 6, 7 , and 8. The absolute shieldings, σ(**Ll**) or σ(**Lr**) for example, are not expected to be quantitatively reproduced since the calculations were not for the covalently bonded substituents. Only the chiral potentials provided by the **l** and **r** substituent groups in the appropriate spatial configurations are systematically accurate. We expect to reproduce the sign and the order of magnitude of the diastereomeric shielding differences [σ(**Lr**) − σ(**Ll**)] by the quantum mechanical calculation for Xe at a single specific location within the cage. Although we calculated only Xe shielding responses at a single position within the cage, we expect this, in turn, to be directly related to the average

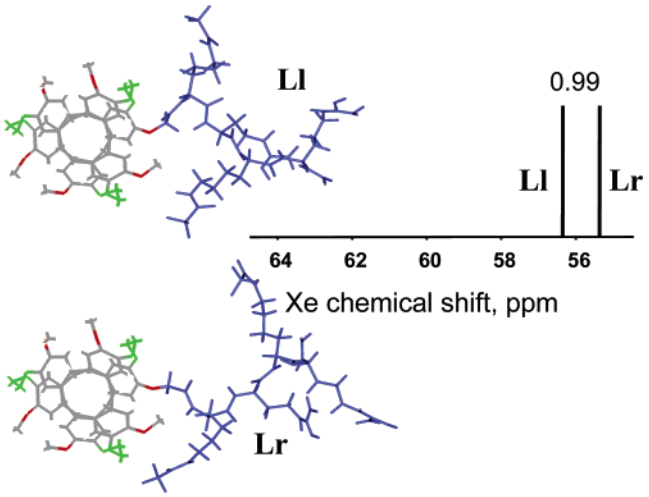

Figure 7. The Xe signals predicted for Xe in the (**L**) cage with (**l**) tether and (**r**) tether attached. The tether in this case is the peptide lysine−arginine−lysine−arginine modified by trifluoroacetic groups. The tether is shown in the conformations for (**l**) and (**r**) forms, respectively, obtained by molecular dynamics simulations of each tethered cage in a solvent box.

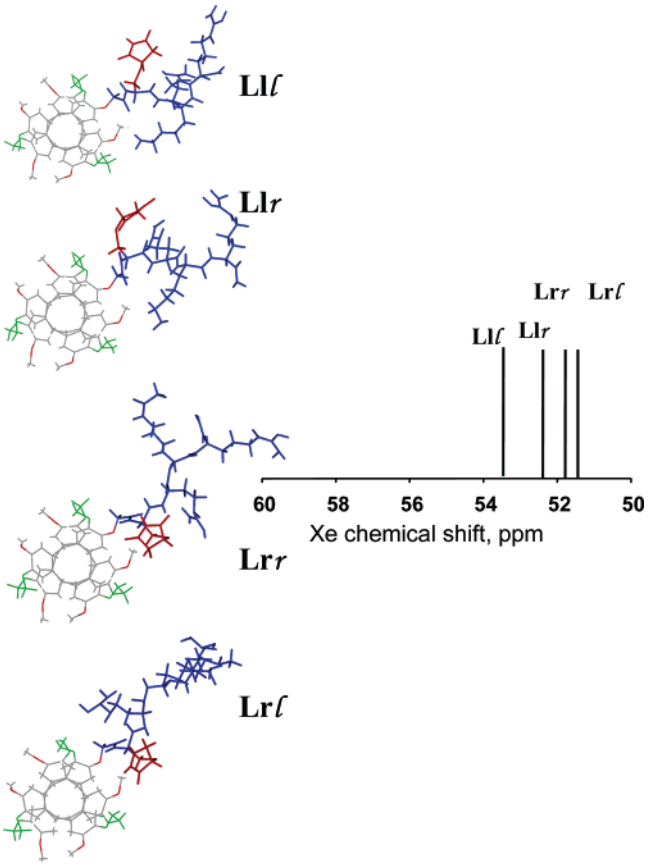

Figure 8. The tethers in this case have the chemical structure of the biosensor shown in Figure 4. The Xe signals predicted for Xe in the four members of the diastereomeric set constituting the biosensor, **Ll***r*, **Lr***ℓ*, **Ll***ℓ*, and **Lr***r*, systems, i.e., the (**L**) cage with four different tethers attached: (**l***r*), (**r***ℓ*), (**l***ℓ*), and (**r***r*). The tether is shown in the conformations for the four forms respectively, obtained by molecular dynamics simulations of each biosensor in a solvent box. The structures shown here are the ones actually used for the quantum calculations of Xe shielding; the linker-biotin pieces have been clipped off.

diastereomeric splittings [δ(**Ll**) − δ(**Lr**)] which are observed experimentally. In this way we may assign the individual peaks to the appropriate member of the diastereomeric set.

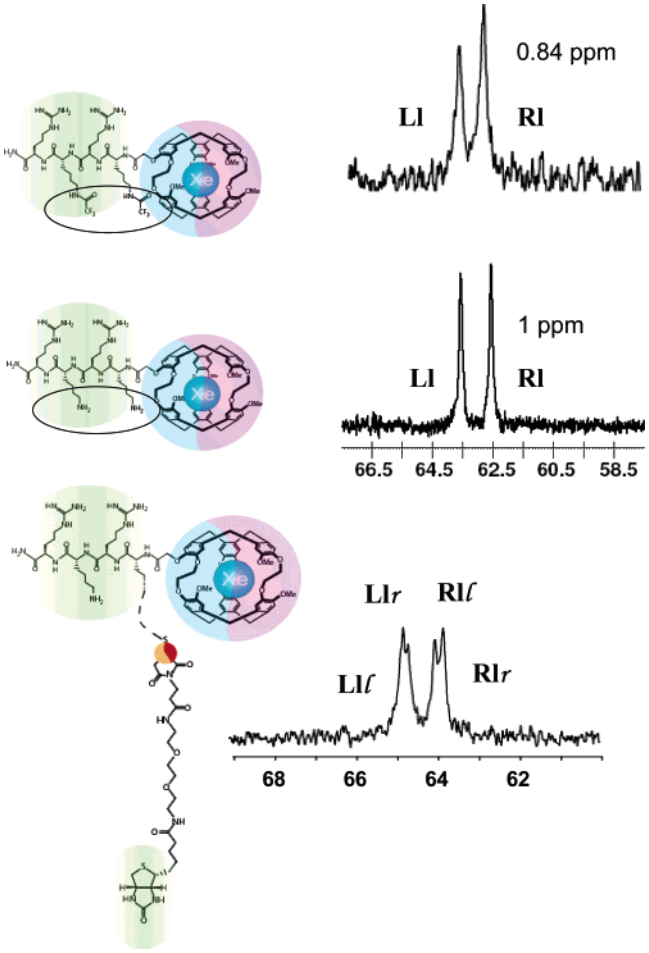

Figure 9. The assignments of the experimental Xe signals to the appropriate members of the diastereomeric set are made possible by the theoretical calculations.

We find in Figure 9 that unequivocal assignments are indeed possible, for the splittings that we obtain are sufficiently large to avoid confusion or round-off errors. It is interesting that the sign of [δ(**Ll**) − δ(**Lr**)] is consistent; that is, we find the like-handed member consistently appears at higher chemical shift, the opposite-handed at lower chemical shift, independent of the tether group.

A distance dependence of the diastereomeric shifts is suggested by the large and small splittings observed in the set of four peaks in the experimental spectra. For systems with more than one asymmetric center in the substituent, it may be possible to deduce the dependence of diastereomeric shifts on the distance of chiral centers from the Xe position. In this example, the maleimide group branches off from the first amino acid residue of the peptide. This puts the chiral center of the maleimide spatially farther away than the chiral center of the first (cysteine) amino acid, although the actual chiral center-to-Xe distances differ by only 3.5 Å on average. In Figure 8, the second letter in the label corresponds to the blue (peptide) part of the tether in the structures, while the third letter corresponds to the red (maleimide) part of the tether. We find in Figure 8 that [δ(**Ll***ℓ*) − δ(**Lr***ℓ*)] is greater than either [δ(**Ll***ℓ*) − δ(**Ll***r*)] or [δ(**Lr***ℓ*) − δ(**Lr***r*)]. Also [δ(**Ll***r*) − δ(**Lr***r*)] > [δ(**Lr***ℓ*) − δ(**Lr***r*)]; that is, the diastereomeric splitting is larger for the blue (closer) asymmetric center and smaller for the red (farther) one. For the diastereomeric set considered here, the through-space

distances of the asymmetric centers to the center of the cage are in the same relative order as the through-bond distances from the site of attachment. Thus, we are unable to distinguish which distances from the Xe position (through-space or through-bond) determine the magnitude of the diastereomeric splitting. Furthermore, the larger distance of the chiral center from the Xe may not be the main reason for the smaller additional splitting induced by the maleimide group. The chiral potential due to the maleimide provides only minor ⁄ or ⁄ perturbations on the larger chiral potential from the all-left-handed or all-right-handed peptide chain. Therefore, we find that we can use the results of the theoretical calculations to assign unequivocally the four peaks observed for the biosensor molecule to the corresponding member of the diastereomeric sets. These assignments are shown in Figure 9. As stated previously, the complete tether in the biosensor structure of Figure 9 differs from that which was used in the quantum calculations. Although the entire biosensor molecule of Figure 9 was used in molecular dynamics simulations in order to find low-energy configurations of the four members of the diastereomeric set, the quantum calculations used the structures shown in Figure 8, which eliminated the linker and the biotin.

V. Discussion

Comparison of Figures 6, 7, and 8 with Figure 9 shows that agreement with experiment is not quantitative. We do not expect quantitative agreement since we have only calculated the Xe shielding response at a single position within the cage; we have not carried out the complete chemical shift averaging overall the probable Xe positions within the cage. Nevertheless, the correspondence between the calculated shielding differences and the observed chemical shift differences is consistent and systematic. This suggests that we have picked a suitably representative position for the Xe atom within the cryptophane-A cage. The primary electronic effects on the cage electronic structure depend on the ability of the specific ligand to withdraw or provide electrons to the parent cage. The modified electronic structure of the cage, in turn, develops a different shielding response at the Xe nucleus. This modified shielding response which is a function of the Xe position within the cage is averaged over Xe@cage−tether nuclear configurations in the real physical system. We do not attempt to reproduce the relative order of Xe chemical shifts from one tether to another. We did not include the all-electron tether atoms in the Xe shielding calculations, so we are unable to predict the chemical shifts from one tether to another. However, all members (two or four) of a given diastereomeric set have the same primary electronic effect on the electronic structure of the cage, since the members of tether sets differ only in chirality. Our goal is to distinguish only the secondary electronic effect that arises from the different spatial arrangements of the same chemical functional groups outside the cage, and this electronic effect is represented by the array of partial charges in the appropriate spatial configuration with respect to the cage.

The approach used in the present work is limited by our assumption that the (**l**) and (**r**) substituents do not result in *differential* mechanical deformation of the cage, so that the Xe would experience the same average internal volume of the cage during the averaging. We could investigate how drastic this approximation is by carrying out a molecular mechanics molecular dynamics simulation in which we compare the Xe-site pair distribution functions for Xe@(**Ll**) against Xe@(**Lr**), where site = C_{ring}, C_{alkyl}, $C_{methoxy}$, and O. However, there are two pieces of experimental evidence relating to cage dynamics which indicate diastereomeric shifts are not greatly influenced by *differential* mechanical deformation of the cage. The first indication of this is a lack of change in the splitting with temperature. It was observed in variable temperature experiments reported elsewhere by Lowery et al. [24] that the absolute positions of the functionalized chemical shifts change linearly with temperature, yielding a temperature coefficient of 0.27 ppm/K. It was observed that the peaks of the diastereomers move in pairs to their new chemical shift positions as dictated by the temperature. For an increase of 15 K in temperature, only a 0.2 ppm decrease in diastereomeric splitting was observed. The second indication of the weak participation of mechanical effects in the diastereomeric splitting comes from a comparison of deuterated and protonated biosensors. When the cage molecule was deuterated at all the bridge sites, the diastereomeric splitting was unaffected. The most extreme case of mechanical deformation is likely for the sensor bound to the protein. Nevertheless, it has been shown that the chemical shift order of the twin peaks is preserved upon binding, although each peak shifts independently of the other.[24] On the other hand, in the case where the distance between the stereogenic center and the Xe site is small enough such that the chiral substituent affects the dynamics of the atoms of the cage, then differential deformation can indeed cause larger diastereomeric shifts as well as differential Xe binding energies and exchange rates. A dramatic example of such a case has been reported by Berthault and co-workers, Xe in the diastereomeric pair *anti*(−)-cryptophanol A and (−)-camphanic acid chloride and *anti*(+)-cryptophanol A and (−)-camphanic acid chloride.[42]

Of course, experimental assignment of the Xe NMR signals in a diastereomeric precursor to **Rl** and **Ll** respectively would be unequivocal if the **R** or **L** cage could be synthesized with enantiomeric purity or if the racemic mixtures could be partially resolved prior to functionalization with **l**. Brotin et al. have recently synthesized optically pure (**R**) cryptophane-A and optically pure (**R**) cryptophanol-A.[36] The latter provide synthetic access to new enantiopure functionalized cryptophanes with host−guest properties similar to those of cryptophane-A. Xenon NMR spectra in partially enantiomerically resolved precursors would verify the validity of the theoretical assignments made in the present work. Furthermore, there is an advantage to using optically pure cage syntheses in the planned multiplexed applications of Xe biosensors; reducing the number of Xe signals to a single one for each sensor would lead to less crowded spectra with better signal-to-noise ratios.

VI. Conclusions

The quantum mechanical values of isotropic Xe shielding responses in the present work permit the prediction of the Xe NMR spectrum in solutions containing the diastereomeric systems resulting from chiral substituents attached to chiral cages. We have demonstrated that the different chiral potentials of the **l** and the **r** enantiomers of the substituent group lead to theoretically different Xe shielding responses for the xenon atom within the **L** cage. The difference in the Xe shielding response

(42) Huber, J. G.; Dubois, L.; Desvaux, H. ; Dutasta, J.-P.; Brotin, T.; Berthault, P. *J. Phys. Chem. A* **2004**, *108*, 9608−9615.

at a single selected Xe location within the cage is sufficient to provide the prediction of the relative order of the *average* Xe chemical shifts, on the basis of the assumption that the one-body distribution function for Xe within the cage is the same for **Lr** and **Ll** systems. This assumption neglects differential mechanical deformation of the cage in the diastereomers. We had found in our previous work on Xe in diastereomeric helices that both geometry and chirality matter.[30] In the present work we employed molecular dynamic simulations of the **Lr** and **Ll** systems in a solvent in order to have the correct spatial geometry of the **r** and **l** substituents with respect to the cage. Thus, for each diastereomeric set, we can confidently assert in which one of the **Lr** and **Ll** systems the Xe atom has the higher chemical shift. The analogous experimental physical systems are **Ll** and **Rl** (mirror image of **Lr**). The higher chemical shift corresponds to the like-handed and the lower chemical shift to the opposite-handed diastereomers. Therefore, in a very real sense, the **l** substituent acts as an experimental probe of the chirality of the Xe@cage. The magnitude of the splitting does vary depending on the substituent. We do not reproduce the relative magnitudes of the diastereomeric splittings for the various tethers we employed since only single point shielding calculations were carried out. For a more complete theoretical analysis, one would need to carry out an ab initio calculation of the entire Xe shielding surface and perform the complete dynamic averaging of the Xe shielding over all Xe, cage, and tether atom positions.

We may extend our findings to the effects of binding on the diastereomeric splittings. The differential average arrangement of the tether around an **L** or **R** cage arises from the different fit or drape of the tether with respect to the **L** and **R** cages. Buffeting of the cage against the protein surface may change the average positions of cage and tether atoms but does not alter the qualitative nature of the drape. Thus, the two peaks should move more or less in tandem, with mechanical averaging providing some alteration of the splitting upon binding to the protein.

Calculations on a set of four Xe-distinguishable systems, the **Lr**$_{r}$, **Llr**$_{r}$, **Lr**$_{l}$, and **Ll**$_{l}$ systems, permit the ordering of the Xe shielding responses and Xe chemical shifts of the **Rl**$_{l}$, **Ll**$_{r}$, **Rl**$_{r}$, and **Ll**$_{l}$ experimental physical systems, respectively. In these sets, the substituents have identical electronic structure, except for the handedness of the asymmetric centers, so it is possible to discern the effect of the remoteness of the asymmetric center from the cage; in these systems, the distance between the center of the cage and the asymmetric center in the substituent does appear to be a factor.

Acknowledgment. We thank Robert A. Harris for discussions about chirality in general and diastereomeric splittings in particular. This research was funded in part by the National Science Foundation (Grant CHE-9979259). C.J.J. is grateful to the Miller Research Foundation for a Visiting Research Professorship at University of California at Berkeley, during which time her work became motivated and inspired by the biosensor applications proposed by Alex Pines, David Wemmer, and their research groups. E.J.R. acknowledges Lucent Technologies/Bell Laboratories for a predoctoral fellowship. This work was supported by the Director, Office of Science, Office of Basic Energy Sciences, and Materials Sciences Division of the U.S. Department of Energy under Contract No. DE-AC03-76SF00098.

JA066661Z